

# Design of Triple Band U-Slot MIMO Antenna for Simultaneous Uplink and Downlink Communications

Jangampally Rajeshwar Goud<sup>1, \*</sup>,  
Nalam V. Koteswara Rao<sup>2</sup>, and Avala Mallikarjuna Prasad<sup>3</sup>

**Abstract**—In this paper, two microstrip antennas with a U-slot on the patch are presented for base station applications to provide simultaneous communications for uplink and downlink, respectively. The intended antennas are expected to operate in triple bands, i.e., to cover GSM and LTE bands. The three designated bands for uplink antenna are from 823 MHz to 830 MHz for lower band, 1.738 GHz to 1.761 GHz for middle band, and 2.321 GHz to 2.355 GHz for upper band. Similarly, the antenna which is designed for downlink operates in three bands from 872 MHz to 880 MHz for lower band, 1.81 GHz to 1.85 GHz for middle band, and 2.338 GHz to 2.375 GHz for upper band. These frequency band(s) satisfy the requirements of GSM850, GSM1800, and LTE2300 bands. Comparisons among designed, simulated, and measured results are presented. Isolation parameters and the Envelope Correlation Coefficient (ECC) values of Multiple Input Multiple Output (MIMO) antenna in all specified bands are also presented.

## 1. INTRODUCTION

Utilization of various wireless mobile communication technologies is increasing day-by-day, and available radio spectrum is limited. In general, different mobile network providers use separate base station antennas to cover GSM850 band, GSM1800, and LTE2300 bands. Traditionally, in light of the fact that a single antenna cannot work at all of these frequency bands of mobile communication, various antennas covering these bands independently ought to be utilized. Notwithstanding, the utilization of numerous antennas is generally restricted by the volume and cost limitations of the applications. Therefore, multiband MIMO antennas are required for wireless mobile communication. There are different kinds of broadband antennas focused on these base station applications, Global System for Mobile communications (GSM850/900/1800/1900), DCS, PCS, UMTS, Long Term Evaluation (2300/2500/2600) in the writing, including patch reception apparatuses [1, 2], magneto-electric dipoles [3, 4], trapezoidal dipoles [5], folded monopole [6], tapered slot [7], and couple of folded dipoles [8]. Multi broadband antennas are used for base station applications, which can receive unwanted frequencies except if some of the filtering systems are acquainted with rejecting such frequencies. Multiband frequency configuration is that it concentrates just on the frequencies of intrigue [9]. Hence, there is high demand to design multi narrow band MIMO antennas for base stations.

Existing models like triple narrow bands using three individual meander-line-type converted-L radiators [10], couple of arc slots [11], U-slot design [12], and two meander lines [13] have a few disadvantages as they require guard period, guard band, and intermittent carrying to segregate uplink and downlink communications. Additionally, base stations should be synchronized for uplink and

---

*Received 24 August 2020, Accepted 12 November 2020, Scheduled 23 November 2020*

\* Corresponding author: Jangampally Rajeshwar Goud (rajeshwargoud@gmail.com).

<sup>1</sup> ECE Dept., Jawaharlal Nehru Technological University, Kakinada, Andhra Pradesh, India. <sup>2</sup> ECE Dept., Chaitanya Bharathi Institute of Technology, Hyderabad, Telangana, India. <sup>3</sup> ECE Dept., University College of Engineering, Jawaharlal Nehru Technological University, Kakinada, Andhra Pradesh, India.

downlink communications to avoid interference [14]. To defeat these drawbacks, there is a significant necessity for a novel antenna design that allows simultaneous communication between transmission and reception using multiple narrow bands.

To meet the requirement, triple band U slot uplink and downlink antennas have been designed which find applications in GSM850, GSM1800 and LTE2300 bands. The proposed antenna geometry, development, and analysis of resonance frequencies are presented. Effect of antenna dimensions and slot positions on resonance frequencies is explained. Simulated and measured antenna parameters are explained in next sections. Simulated results of the proposed MIMO antennas are also presented.

## 2. ANTENNA STRUCTURE AND DEVELOPMENT

The proposed structure and fabricated antennas are shown in Figure 1. The triple band inset feed U slot uplink and downlink antennas are designed to cover GSM850, GSM1800, and LTE2300 frequency bands having dimensions of FR4 substrate length and width  $70 \text{ mm} \times 130 \text{ mm}$  and height ( $h$ )  $1.6 \text{ mm}$  with  $\epsilon_r = 4.4$ . To obtain simultaneous communication for uplink and downlink, two separate triple band U antennas are designed on single substrate in which one can be used for uplink and the other for downlink communication. These three bands can be achieved by providing slots on the patch, in which two horizontal slots ( $S_{L2}$ ) are positioned symmetrically with respect to the feed and vertical slot ( $S_{L1}$ ) in between horizontal slots which forms U slot structure and is shown in Figure 1. To meet the requirement of MIMO system, at least two antennas should work on same frequencies. For this purpose, other uplink and downlink antennas are added adjacent to the existing antennas, and hence the proposed MIMO antenna size becomes length ( $L_g$ )  $70 \text{ mm}$ , width ( $W_g$ )  $240 \text{ mm}$ , height ( $h$ )  $1.6 \text{ mm}$ , which are shown in Figure 2(a). To improve the performance of MIMO antenna, uplink and downlink antennas are arranged alternately and are shown in Figures 2(b) and 2(c). All the antennas operate with individual ports. In prototype-I, ports 1 and 2 are assigned for downlink purpose and ports 3 and 4 for uplink. Similarly in prototype-II and III, ports 1 and 3 are assigned for uplink purpose and ports 2 and 4 for downlink. For impedance matching, each antenna is designed with a  $50 \Omega$  strip line.

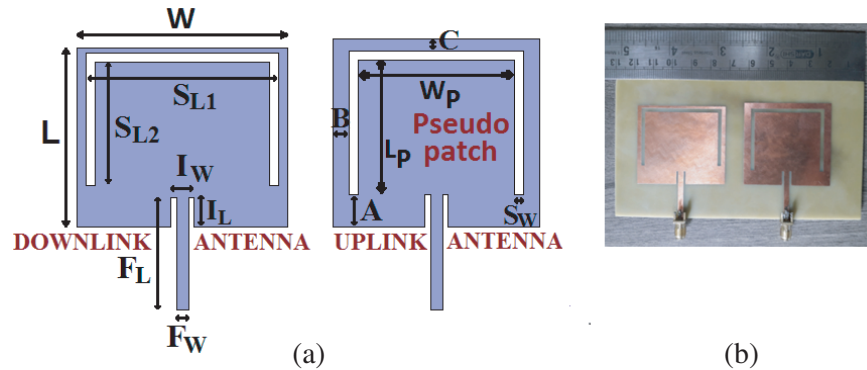


**Figure 1.** Triple band inset feed U slot antennas (a) Geometry (b) fabricated antenna.

### 2.1. Development and Analysis of the Resonance frequencies

This proposed antenna is useful for 2G, 3G, and 4G mobile applications, which covers GSM850, GSM1800, and LTE2300 bands. The provision of slots on the patch will generate multiple frequencies. These slots alter the current paths of plain patch. Variations in surface current distributions of downlink antennas with and without a U slot are shown in Figure 12. Similarly, the same effect will take place in uplink antennas. The variations of slot positions (i.e., A, B, and C), length and width of the slots, height of the substrate, length ( $L$ ) and width ( $W$ ) of the patch and effective dielectric constant cause changes in resonance frequencies. However, these changes will not show equal impact on all resonance frequencies. Detailed comparisons of parameter variations are clarified in next section. The inset feed lengths ( $F_L$ ) and feed widths ( $F_W$ ) have no significant impact on resonance frequencies. The design

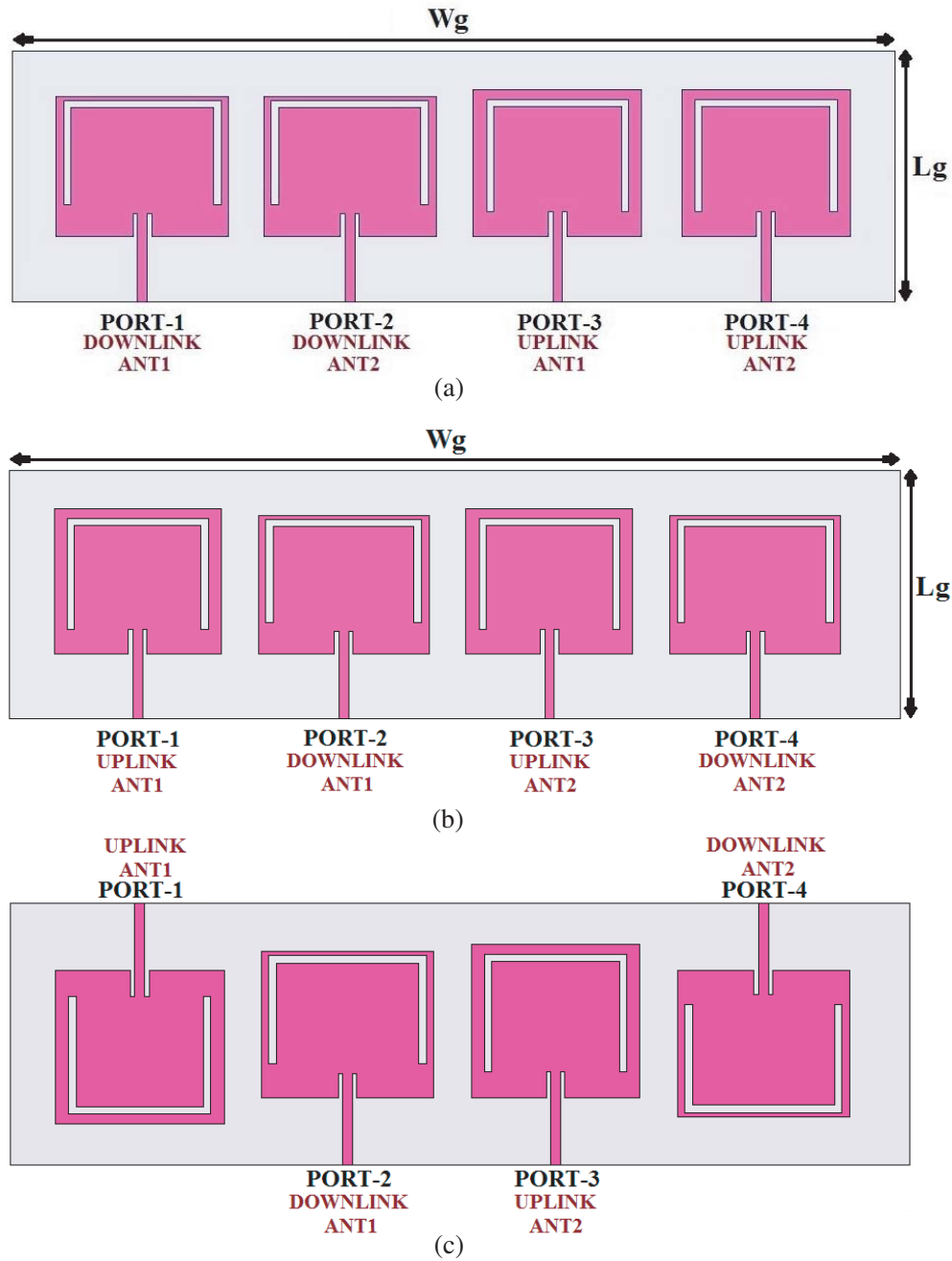


**Figure 2.** Triple band inset feed U slot MIMO antenna. (a) Prototype-I. (b) Prototype-II. (c) Prototype-III.

formulas which are proposed in [15] and [16] are required to be optimized for microstrip line fed thin substrate structures. However, design dimensions are optimized using HFSS, and better expressions are presented for microstrip line fed thin substrate structures. The analytical expressions for the resonance frequencies  $f_{res1}$ ,  $f_{res2}$ , and  $f_{res3}$  are given below.

2.1.1. First Resonant Frequency ( $f_{res1}$ )

$f_{res1}$  depends upon patch length, vertical slot length ' $S_{L1}$ ', horizontal slot length ' $S_{L2}$ ', and positions of the U slot. Horizontal slot is proportional to the positions A, C, and vertical slot width ' $S_W$ '. This

resonant frequency decreases by increasing the slot length, width, and position 'C'.  $f_{res1}$  increases by increasing positions 'A' and 'B'. This resonant frequency will be lower than that of the plain patch since the U-slot alters the usual current paths of main radiating edges. The overall electrical patch length increases by providing slots at edges of the patch, hence the resonant frequency falls in the lower band. The estimated expression of  $f_{res1}$  is given below.

$$f_{res1} = \frac{v_0}{2 \left( \sqrt{\epsilon_{eff}} \right) \left( L + 2\Delta L + \frac{(S_{L1} - A)}{2} + S_{L2} + S_W + C - B \right)} \quad (1)$$

### 2.1.2. Second Resonant Frequency ( $f_{res2}$ )

This resonance frequency strongly depends on the patch length whose length is equal to half wavelength without U slot on the patch. However, slot dimensions and positions on patch will affect this resonance frequency. The impact of position 'A' on this frequency is negligible since it mainly depends on the patch length. This resonant frequency increases by increasing position 'C', slot width ' $S_W$ ', and decreasing position 'B'. It also depends on the ratio of the horizontal and vertical slot lengths. The estimated equation of  $f_{res2}$  is given below.

$$f_{res2} = \frac{v_0}{2 \left( \sqrt{\epsilon_{eff}} \right) \left( L + 2\Delta L + \frac{2S_{L2}}{S_{L1}} + B - S_W - C \right)} \quad (2)$$

where  $v_0$  is the light velocity

$$\epsilon_{eff} = \frac{\epsilon_r + 1}{2} + \frac{\epsilon_r - 1}{2} \left[ 1 + 12 \frac{h}{W} \right]^{-\frac{1}{2}} \quad (3)$$

$$\Delta L = 0.412h \left[ \frac{(\epsilon_{eff} + 0.3) \left( \frac{W}{h} + 0.264 \right)}{(\epsilon_{eff} - 0.258) \left( \frac{W}{h} + 0.8 \right)} \right] \quad (4)$$

### 2.1.3. Third Resonant Frequency ( $f_{res3}$ )

A pseudo patch (PP) with length ( $L_P$ ) and width ( $W_P$ ) is created by providing the U slot on the main patch which is shown in Figure 1. The dimensions of the pseudo patch will determine this resonant frequency.  $f_{res3}$  increases by increasing positions 'B' and 'C' and slot width ' $S_W$ '. The effect of position 'A' on this resonant frequency is less than 'B' and 'C' due to the U slot. The estimated expression of  $f_{res3}$  is given below.

$$f_{res3} = \frac{v_0}{2 \left( \sqrt{\epsilon_{eff(PP)}} \right) \left( L_P + 2\Delta L_P + \frac{A}{2} - \frac{S_{L2}}{2A} \right)} \quad (5)$$

$$\epsilon_{eff(PP)} = \frac{\epsilon_r + 1}{2} + \frac{\epsilon_r - 1}{2} \left[ 1 + 12 \frac{h}{W_P} \right]^{-\frac{1}{2}} \quad (6)$$

$$\Delta L_P = 0.412h \left[ \frac{(\epsilon_{eff(PP)} + 0.3) \left( \frac{W_P}{h} + 0.264 \right)}{(\epsilon_{eff(PP)} - 0.258) \left( \frac{W_P}{h} + 0.8 \right)} \right] \quad (7)$$

where  $W_P = W - 2B - 2S_W$  and  $L_P = L - A - C - S_W$ .

### 2.2. Effect of Antenna Dimensions and Slot Positions on Resonant Frequencies

The resonance frequencies mainly depend on the dimensions of slots and slot positions, i.e., ‘A’, ‘B’, and ‘C’ where ‘A’ is the distance from radiating bottom edge, ‘B’ the distance from non-radiating edges, and ‘C’ the distance from radiating top edge. The change in positions ‘A’, ‘B’, and ‘C’ will change the dimensions of vertical slot length ‘ $S_{L1}$ ’ and horizontal slot length ( $S_{L2}$ ) which in turn change the dimensions of pseudo patch. These variations will alter the current paths on the main patch which affects the resonance frequencies. However, not all the parameters show the same effect on resonance frequencies. Variation on each parameter with step size of 0.5 mm shows different effects on individual resonance frequencies which is explained in detail as follows.

#### 2.2.1. Slot Position ‘A’

With the increment of 0.5 mm on slot position ‘A’, proportionally there is an increment of 6 MHz and 13 MHz on the first and third resonance frequencies, respectively. Differentiating simulated and computed results utmost 16 MHz of variation is obtained on first resonance frequency and 26 MHz on the third for both uplink and downlink antennas. The change in slot position ‘A’ will change the length of the pseudo patch. Slot position ‘A’ will have minimal effect on the second resonant frequency. The varied resonance frequencies are illustrated in Figure 3.

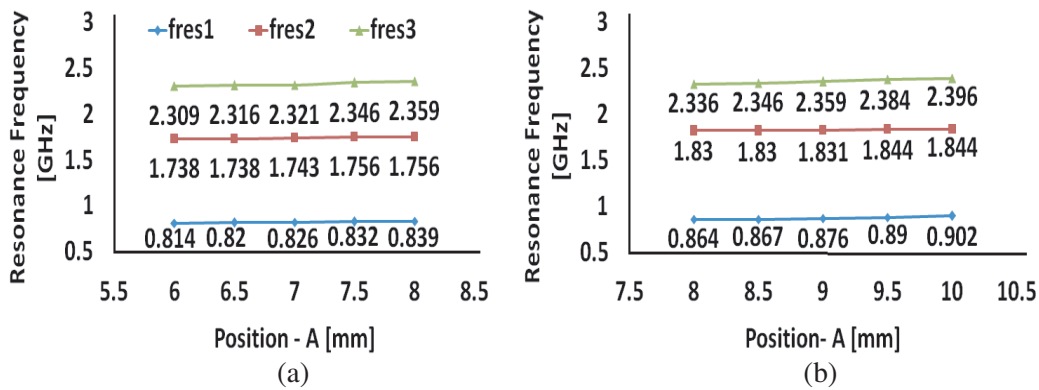


**Figure 3.** Effect of position ‘A’ on resonance frequencies. (a) Uplink antenna. (b) Downlink antenna.

#### 2.2.2. Slot Position ‘B’

With the increment of 0.5 mm on slot position ‘B’, proportionally there is an increment of 28 MHz and 23 MHz on the first and third resonance frequencies, respectively, and decrement of 25 MHz on the second resonance frequency. Differentiating simulated and computed results utmost 33 MHz of variation is obtained on the first resonance frequency, 18 MHz on the second, and 11 MHz on the third for both uplink and downlink antennas. The change in slot position ‘B’ will change the length of the vertical slot length ‘ $S_{L1}$ ’. This will affect all the resonance frequencies. The varied resonance frequencies are illustrated in Figure 4.

#### 2.2.3. Slot Position ‘C’

With the increment of 0.5 mm on slot position ‘C’, proportionally there is an increment of 26 MHz and 27 MHz on the second and third resonance frequencies, respectively, and decrement of 14 MHz on the first resonance frequency. Differentiating simulated and computed results utmost 18 MHz of variation is obtained on the first resonance frequency, 16 MHz on the second, and 13 MHz on the third for both uplink and downlink antennas. The change in slot position ‘C’ will change the length of the pseudo patch. All the resonance frequencies are affected by slot position ‘C’. The varied resonance frequencies are illustrated in Figure 5.

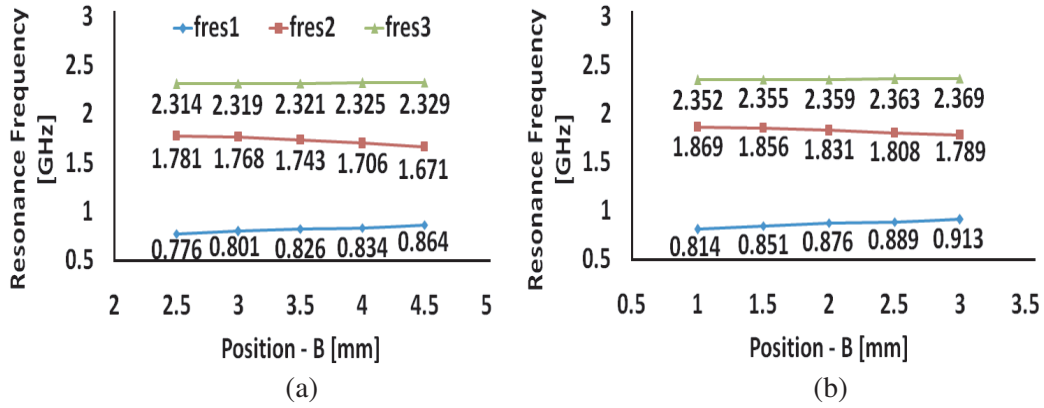


Figure 4. Effect of position ‘B’ on resonant frequencies. (a) Uplink antenna. (b) Downlink antenna.

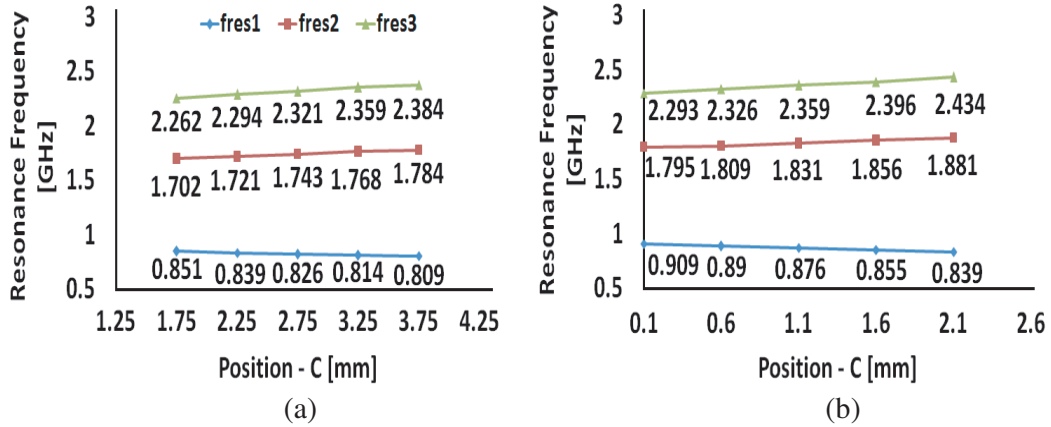


Figure 5. Effect of position ‘C’ on resonant frequencies. (a) Uplink antenna. (b) Downlink antenna.

2.2.4. Slot Width ‘ $S_W$ ’

With the increment of 0.5 mm on slot width ‘ $S_W$ ’, proportionally there is an increment of 26 MHz and 32 MHz on the second and third resonance frequencies, respectively. Differentiating simulated and computed results utmost 17 MHz of variation is obtained on the second resonance frequency and 13 MHz on the third for both uplink and downlink antennas. The first resonant frequency does not change appreciably with changes in slot width ‘ $S_W$ ’. The same width is considered for all the slots. The varied resonance frequencies are illustrated in Figure 6.

Desired resonance frequencies are obtained by selecting suitable dimensions of U slot and patch using design equations and parametric study. Correspondingly, one can easily select suitable dimensions for any application and get desired resonance frequencies with the help of explanation given in this section regarding how resonance frequencies are affected by antenna dimensions and slot positions. The proposed antenna dimensions appear in Table 1.

3. RESULTS AND DISCUSSION

The uplink antenna is designed to cover GSM850 band from 821 MHz to 830 MHz, and return loss –22.26 dB is shown in Figure 7. All other parameters of the proposed antennas are listed in Table 2. Gain versus frequency of uplink and downlink antennas is shown in Figure 8. Gain patterns of uplink and downlink antennas are almost symmetrical for the specified three bands as shown in Figure 9 and Figure 10.

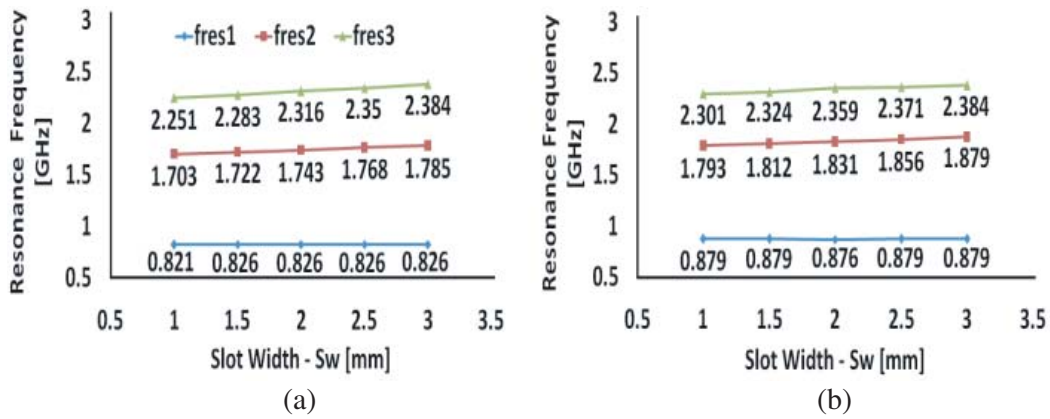


Figure 6. Effect of slot width ' $S_W$ ' on resonant frequencies. (a) Uplink antenna. (b) Downlink antenna.

Table 1. Antenna dimensions.

Parameter	Triple band inset feed U slot uplink antenna (mm)	Triple band inset feed U slot downlink antenna (mm)
L	41	39
W	45	46
$F_L$	25	24.5
$F_W$	2.6	2.65
$I_L$	7	6.5
$I_W$	5	5
$S_{L1}$	38	42
$S_{L2}$	29.25	26.9
$S_{L3}$	29.25	26.9
$S_W$	2	2
A	7	9
B	3.5	2
C	2.75	1.1

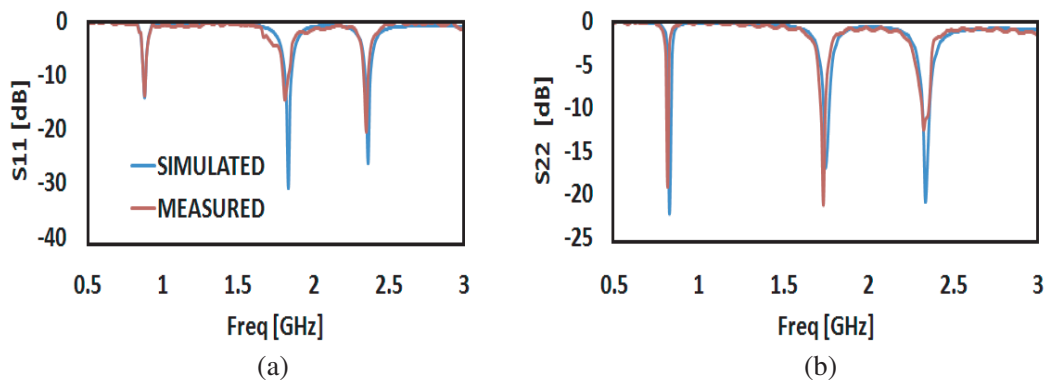
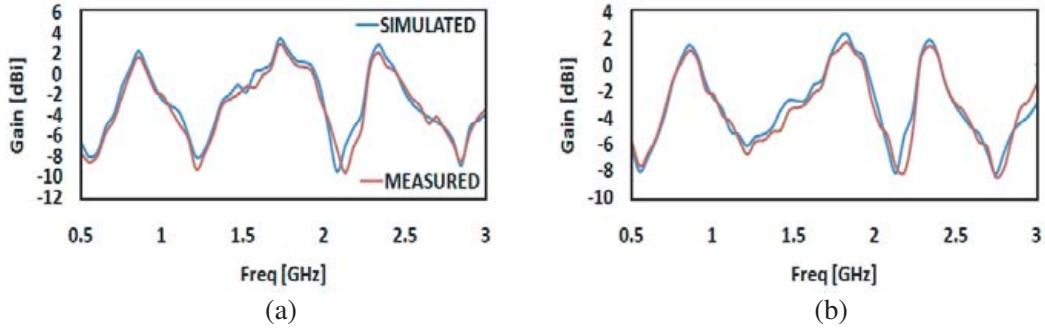
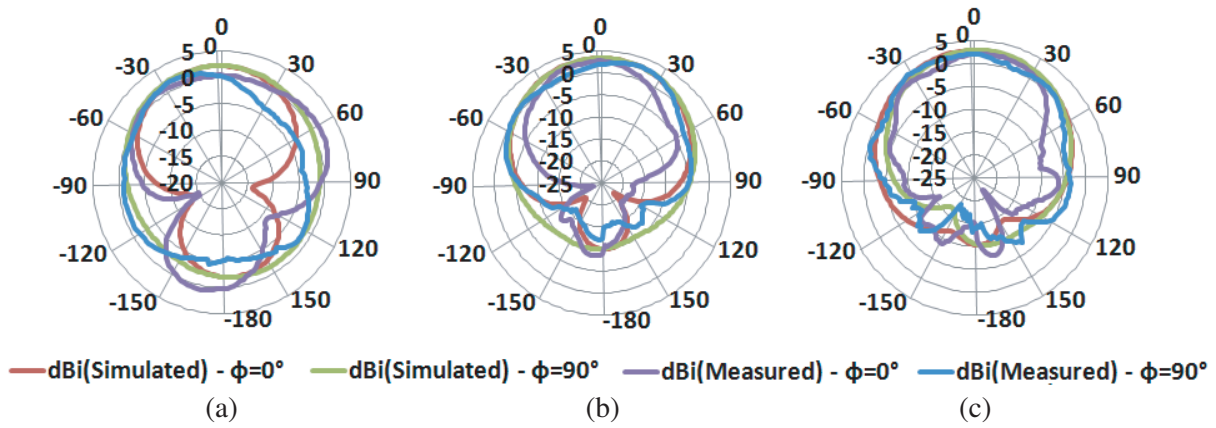


Figure 7. Return loss of a triple band inset feed U slot antenna. (a) Downlink antenna. (b) Uplink antenna.





**Figure 8.** Gain versus frequency of triple band inset feed U slot antenna. (a) Uplink antenna. (b) Downlink antenna.



**Figure 9.** Radiation patterns of a triple band inset feed U slot uplink antenna. (a) Lower band. (b) Middle band. (c) Upper band.

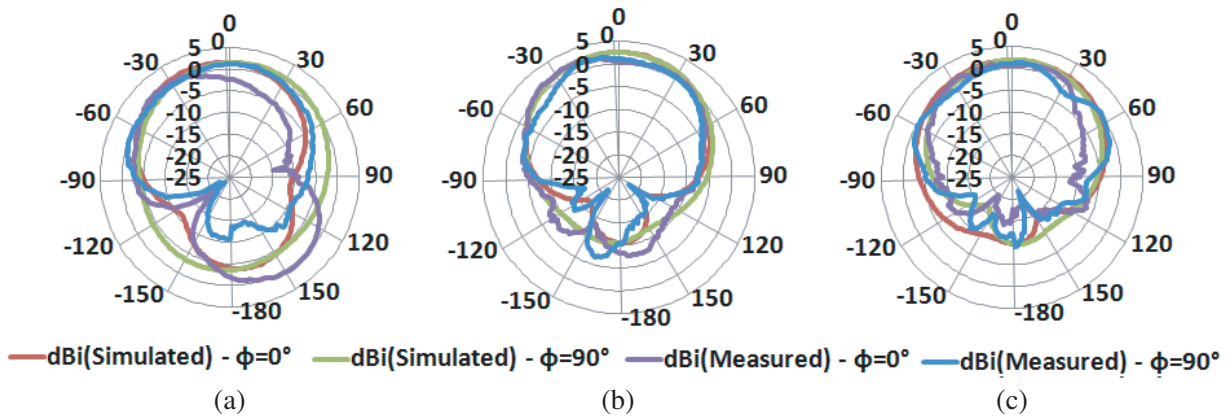


**Figure 10.** Radiation patterns of a triple band inset feed U slot downlink antenna. (a) Lower band. (b) Middle band. (c) Upper band.

The mutual couplings between the ports, i.e.,  $S_{12}$  and  $S_{21}$ , of simulation and measurement are shown in Figure 11. More than 25 dB mutual coupling is obtained for simulation and 20 dB for measurement. Increasing the spacing between the antennas can reduce the mutual coupling which is shown in Figure 11. Spacing between the uplink and downlink antennas is considered  $0.33\lambda$  (port 1 to port 2), where  $\lambda$  is the operating wavelength. The results show that the proposed antenna will provide better isolation for



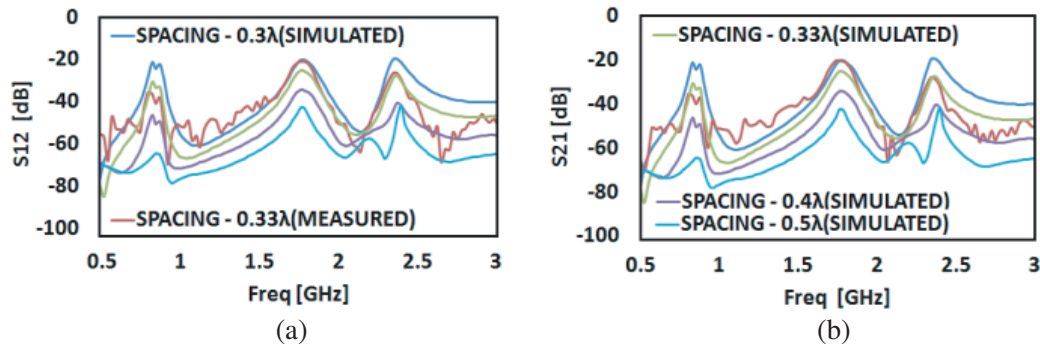


Figure 11. Mutual coupling between the elements (a)  $S_{12}$ , (b)  $S_{21}$ .

Table 2. Antenna parameters.

Parameter	Band	Uplink antenna (Simulated)	Uplink antenna (Measured)	Downlink antenna (Simulated)	Downlink antenna (Measured)
Return loss (dB)	Lower	-22.26	-19.21	-14.09	-13.68
	Middle	-16.84	-21.28	-30.97	-14.39
	Upper	-20.90	-12.56	-26.30	-20.39
VSWR	Lower	1.16	1.24	1.49	1.82
	Middle	1.33	1.61	1.05	1.47
	Upper	1.19	1.18	1.10	1.21
Bandwidth (MHz)	Lower	821–830	812–820	872–880	871–879
	Middle	1738–1761	1715–1745	1810–1850	1801–1842
	Upper	2321–2355	2311–2348	2338–2375	2331–2359
Resonance Frequency (MHz)	Lower	826	814	876	875
	Middle	1743	1731	1831	1815
	Upper	2339	2331	2356	2346
Radiation Efficiency (%)	Lower	36.78	35.95	35.26	34.68
	Middle	41.56	40.39	40.12	37.87
	Upper	38.15	37.82	37.54	36.73
Peak Gain (dBi)	Lower	2.26	1.71	1.62	1.13
	Middle	3.42	2.96	2.36	1.74
	Upper	2.84	2.13	1.95	1.46

uplink and downlink communications. Diversity performance of the proposed antenna is explained in next section.

Bandwidths of uplink and downlink antennas are listed in Table 3. The obtained bandwidth for uplink antenna is 9 MHz, 23 MHz, and 34 MHz, and downlink antenna is operated with 8 MHz, 40 MHz, and 37 MHz lower, middle, and upper resonance bands, respectively, which are sufficient for base station applications [17]. The proposed antenna can provide better isolation for uplink and downlink communications with these narrow bands.

The proposed antenna operates separately for uplink and downlink communications since it consists of separate antennas. Utilizing this strategy, fast switching is conceivable between uplink and downlink communications [14]. Subsequently uplink and downlink triple band U slot antennas are used to provide

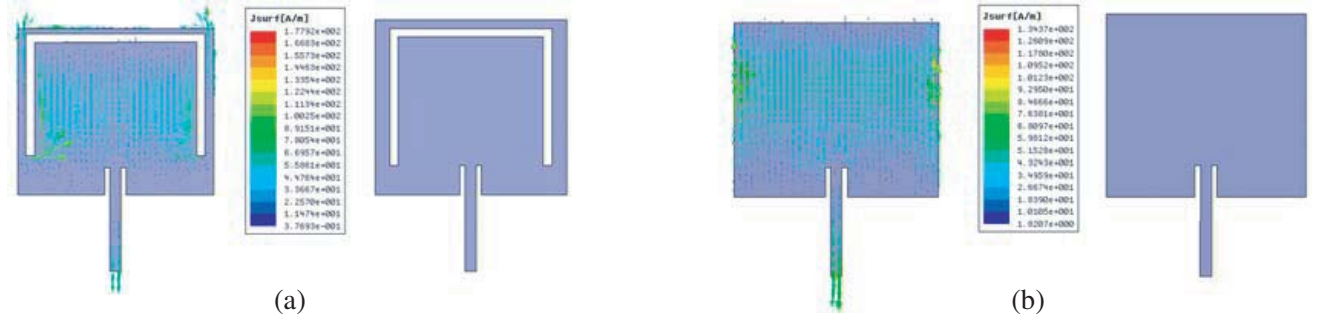


**Figure 12.** Surface current distributions of downlink antennas (a) with U slot and (b) without U slot antennas.

**Table 3.** Comparison with other patch antennas.

Ref.	Size (mm) ( $L \times W \times h$ )	$f_1$ (MHz)	$f_2$ (MHz)	$f_3$ (MHz)	$BW_1$ (MHz)	$BW_2$ (MHz)	$BW_3$ (MHz)	Gain (dBi)
[10]	$100 \times 65 \times 1.6$	900	1800	2600	40	30	170	$f_1$ : 0.25, $f_2$ : 0.60 and $f_3$ : 3.28
[11]	$93 \times 93 \times 3$	830	1800	2460	6	27	18	$f_1$ : 3.1, $f_2$ : 4.4 and $f_3$ : 2.0
[13]	$42 \times 15 \times 1.6$	900	1800	2400	30	40	30	$f_1$ : 1.62, $f_2$ : 2.12 and $f_3$ : 1.89
Proposed	$70 \times 130 \times 1.6$	$f_{1U}$ : 826	$f_{2U}$ : 1743	$f_{3U}$ : 2339	$BW_{1U}$ : 9	$BW_{2U}$ : 23	$BW_{3U}$ : 34	$f_{1U}$ : 2.26, $f_{2U}$ : 3.42 and $f_{3U}$ : 2.84
		$f_{1D}$ : 876	$f_{2D}$ : 1831	$f_{3D}$ : 2356	$BW_{1D}$ : 8	$BW_{2D}$ : 40	$BW_{3D}$ : 37	$f_{1D}$ : 1.62, $f_{2D}$ : 2.36 and $f_{3D}$ : 1.95

simultaneous communication for same as well as various mobile network users. Great relationship is obtained between simulation and measured results.

#### 4. DIVERSITY PERFORMANCE

ECC is a measure that describes how much the communication channels are isolated or related with one another. ECC can be determined utilizing the strategy proposed in [18].

$$ECC(\rho_e) = \frac{|S_{ii}^* S_{ij} + S_{ji}^* S_{jj}|^2}{(1 - |S_{ii}|^2 - |S_{ji}|^2)(1 - |S_{jj}|^2 - |S_{ij}|^2)} \quad (8)$$

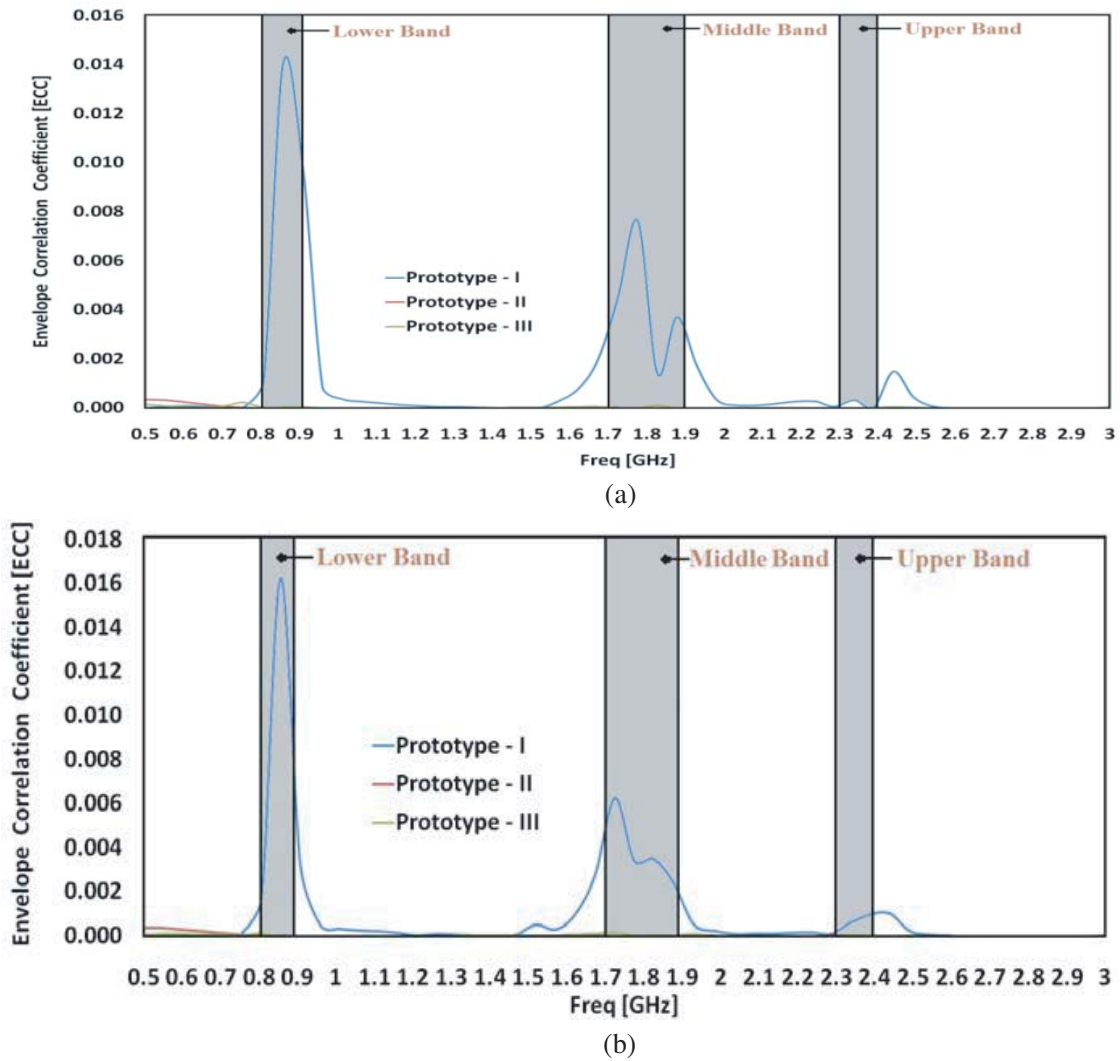


**Figure 13.** ECC of (a) uplink and (b) downlink antennas.

The envelope correlation coefficient (ECC) values of uplink and downlink antennas are shown in Figure 13. The ECC values of proposed antenna prototypes I, II, and III are shown in Table 4. The distance  $0.33\lambda$  is considered between uplink antennas (i.e., from port-3 to port-4) of prototype I whereas  $0.66\lambda$  distance is considered for prototype II and III uplink antennas (i.e., from port-1 to port-3). The distance for downlink antennas is considered same as above. The ECC values are less than 0.016 in all specified bands of uplink and downlink antennas of prototype I and less than 0.00017 in all specified bands of uplink and downlink antennas of prototypes II and III. More than 9.9 dBi diversity gain is

**Table 4.** ECC values of uplink and downlink antennas.

Prototype	UPLINK			DOWNLINK		
	Lower Band	Middle Band	Upper Band	Lower Band	Middle Band	Upper Band
I	< 0.014	< 0.0076	< 0.0003	< 0.016	< 0.0062	< 0.00097
II	< 0.000013	< 0.0001	< 0.00008	< 0.000011	< 0.00017	< 0.000017
III	< 0.000054	< 0.000097	< 0.000013	< 0.00014	< 0.00016	< 0.0000067

obtained for both uplink and downlink antennas using Equation (9). The proposed prototypes II and III provide good diversity performance for MIMO applications. In prototype III, uplink antennas are placed opposite to each other and downlink antennas also placed opposite to each other to provide spatial diversity and to take advantage of polarization diversity.

$$\text{Diversity Gain} = 10\sqrt{1 - |ECC|^2} \quad (9)$$

## 5. CONCLUSION

The uplink and downlink triple band U slot antennas are developed for base stations. These antennas find good applications in GSM850, GSM1800, and LTE2300 bands, which provide simultaneous communications for uplink and downlink. To obtain desired resonance frequencies, the suitable dimensions are chosen based on designed equations and parametric study. The proposed uplink antenna is to operate with 826 MHz, 1.743 GHz, and 2.339 GHz, and downlink antenna is to operate with 876 MHz, 1.831 GHz, and 2.356 GHz lower, middle, and upper resonance frequencies, respectively. Over the entire operating band, the isolation between the two ports is greater than 20 dB which improves the diversity performance. The obtained ECC values and diversity gain of proposed MIMO antenna improve the performance of the MIMO system. Good correlation is obtained between simulation and measured results.

## REFERENCES

1. Wong, K. L., *Planar Antennas for Wireless Communications*, Wiley, New York, 2003.
2. Huang, C. Y. and E. Z. Yu, "A slot-monopole antenna for dual-band WLAN applications," *IEEE Antennas and Wireless Propagation Letters*, Vol. 10, 500–502, 2011.
3. Wu, B. Q. and K. M. Luk, "A broadband dual-polarized magneto-electric dipole antenna with simple feeds," *IEEE Antennas and Wireless Propagation Letters*, Vol. 8, 60–63, 2009.
4. Zhai, H., J. Zhang, Y. Zang, Q. Gao, and C. Liang, "An LTE base-station magnetolectric dipole antenna with anti-interference characteristics and its MIMO system application," *IEEE Antennas and Wireless Propagation Letters*, Vol. 14, 906–909, 2015.
5. An, W. X., H. Wong, K. L. Lau, S. F. Li, and Q. Xue, "Design of broadband dual-band dipole for base station antenna," *IEEE Trans. Antennas Propagat.*, Vol. 60, No. 3, 1592–1595, Mar. 2012.
6. Fang, Q., D. Mi, and Y.-Z. Yin, "A tri-band MIMO antenna for WLAN/WiMAX application," *Progress In Electromagnetics Research Letters*, Vol. 55, 75–80, 2015.
7. Itoh, K., K. Konno, Q. Chen, and S. Inoue, "Design of compact multiband antenna for triple-band cellular base stations," *IEEE Antennas and Wireless Propagation Letters*, Vol. 14, 64–67, 2015.
8. Cui, Y., R. L. Li, and P. Wang, "A novel broadband planar antenna for 2G/3G/LTE base stations," *IEEE Trans. Antennas Propagat.*, Vol. 61, No. 3, 1132–1139, May 2013.
9. Lee, K. F. and K. M. Luk, *Microstrip Patch Antennas*, Imperial College Press, 2011.
10. Sun, J., H. Fang, P. Lin, and C. Chuang, "Triple-band MIMO antenna for mobile wireless applications," *IEEE Antennas and Wireless Propagation Letters*, Vol. 15, 500–503, 2016.
11. Chen, W. K., Y. X. Li, H. Y. Jiang, and Y. L. Long, "Design of novel tri-frequency microstrip patch antenna with arc slots," *Electron. Lett.*, Vol. 48, No. 11, 609–611, May 2012.
12. Rajeshwar Goud, J., N. V. Koteswara Rao, and A. Mallikarjuna Prasad, "Inset feed triple band U-slot antenna for GSM900/GSM1900/WLAN applications," *International Journal of Engineering and Advanced Technology*, Vol. 8, No. 6S3, Sept. 2019.
13. Sun, X.-B., "Design of a triple-band antenna based on its current distribution," *Progress In Electromagnetics Research Letters*, Vol. 90, 113–119, 2020.
14. Holma, H. and A. Toskala, *LTE for UMTS: OFDMA and SC-FDMA Based Radio Access*, 267, John Wiley & Sons Ltd., United Kingdom, 2009.

15. Weigand, S., G. H. Huff, K. H. Pan, and J. T. Bernhard, "Analysis and design of broad-band single-layer rectangular U-slot microstrip patch antennas," *IEEE Trans. Antennas Propagat.*, Vol. 51, No. 3, 457–468, Mar. 2003.
16. Balanis, C. A., *Antenna Theory Analysis and Design*, John Wiley & Sons, Inc., Hoboken, New Jersey, USA, 2005.
17. Mishra, A. R., *Fundamentals of Cellular Network Planning and Optimisation 2G/2.5G/3... Evolution to 4G*, John Wiley & Sons Ltd., 2004
18. Blanch, S., J. Romeu, and I. Corbella, "Exact representation of antenna system diversity performance from input parameter description," *Electron. Lett.*, Vol. 39, No. 9, 70–707, 2003.